Climate Dynamics (1994) 9:287–302

Climate Dynamics

Interdecadal variability of the Pacific Ocean: model response to observed heat flux and wind stress anomalies

Arthur J Miller[1], **Daniel R Cayan**[1], **Tim P Barnett**[1], **Nicholas E Graham**[1], **Josef M Oberhuber**[2]

[1] Scripps Institution of Oceanography, La Jolla, CA 92093-0224, USA
[2] Meteorological Institute, University of Hamburg, Germany

Received: 19 October 1992/Accepted: 13 April 1993

Abstract. Variability of the Pacific Ocean is examined in numerical simulations with an ocean general circulation model forced by observed anomalies of surface heat flux, wind stress and turbulent kinetic energy (TKE) over the period 1970–88. The model captures the 1976–77 winter time climate shift in sea surface temperature, as well as its monthly, seasonal and longer term variability as evidenced in regional time series and empirical orthogonal function analyses. Examination of the surface mixed-layer heat budget reveals that the 1976–77 shift was caused by a unique concurrance of sustained heat flux input anomalies and very strong horizontal advection anomalies during a multi-month period preceding the shift in both the central Pacific region (where cooling occurred) and the California coastal region (where warming occurred). In the central Pacific, the warm conditions preceding and the cold conditions following the shift tend to be maintained by anomalous vertical mixing due to increases in the atmospheric momentum flux (TKE input) into the mixed layer (which deepens in the model after the shift) from the early 1970s to the late 1970s and 1980s. Since the ocean model does not contain feedback to the atmosphere and it succeeds in capturing the major features of the 1976–77 shift, it appears that the midlatitude part of the shift was driven by the atmosphere, although effects of midlatitude ocean-atmosphere feedback are still possible. The surface mixed-layer heat budget also reveals that, in the central Pacific, the effects of heat flux input and vertical mixing anomalies are comparable in amplitude while horizontal advection anomalies are roughly half that size. In the California coastal region, in contrast, where wind variability is much weaker than in the central Pacific, horizontal advection and vertical mixing effects on the mixed-layer heat budget are only one-quarter the size of typical heat flux input anomalies.

1 Introduction

Among the least understood aspects of climate variability are the changes which occur on decadal time scales (e.g., Douglas et al. 1982; Folland et al. 1984; Peixoto and Oort 1992). These regime changes can occur as gradual drifts over many years or as dramatic shifts in less than a year. In order to better understand man's long-term influence on the changing climate system, it is imperative to attempt to identify, diagnose and understand these interdecadal variations of the climate system.

One such shift in the climate system occurred in the Pacific Ocean during 1976–77 (e.g., McLain 1983; Nitta and Yamada 1989; Trenberth 1990; Graham 1991; Ebbesmeyer et al. 1991). Large-scale atmospheric and oceanic changes were first noted as a deepening of the Aleutian Low, a drop in sea surface temperature (SST) in the central Pacific and a rise in SST in the eastern Pacific (Namias 1978; Venrick et al. 1987; Kashiwabara 1987; Nitta and Yamada 1989; Trenberth 1990; Tanimoto et al. 1992; Xu 1992). Other variables which underwent step-like changes in 1976–77 include tropospheric water vapor (Gaffen et al. 1991), zonal winds and chlorophyll-a content (Venrick et al. 1987), and the wave climate along the California coast (Seymour et al. 1984). Ebbesmeyer et al. (1991) composited normalized changes of 40 different variables in demonstrating the significance of the 1976–77 step over a broad array of environmental and biological systems of the north Pacific/western North America areas.

Attention to this particular decadal shift, and others of this type, is crucial to understanding whether long-term changes in the climate system are anthropogenic or naturally induced. To identify greenhouse warming effects, we must be able to discriminate from natural variability in this intermediate low-frequency range. For example, Kashiwabara (1987) suggested that the

This paper was presented at the Second International Conference on Modelling of Global Climate Variability, held in Hamburg 7–11 September 1992 under the auspices of the Max Planck Institute for Meteorology. Guest Editor for these papers is L. Dümenil

Correspondence to: AJ Miller

1976–77 shift in climate in the north Pacific Ocean could, among other mechanisms, be caused by persistently warm SST in the tropical Pacific, which can transmit a signal to the middle latitudes in celebrated fashion (e.g. Bjerknes 1969; Horel and Wallace 1981; Alexander 1990). Nitta and Yamada (1989) subsequently demonstrated that tropical Pacific SST warming, and a commensurate increase in atmospheric convective activity, indeed coincided with the 1976–77 shift. A similar explanation of the tropical origin of the shift was advanced by Trenberth (1990), who suggested that a lack of La Niñas during the late 1970s and early 1980s may have been the primary causal factor. Graham (1991) showed that an atmospheric general circulation model (GCM) forced by observed global SST variations generates a shift in 700 mb heights over the extratropical north Pacific similar to the observed, and suggested that a change in background mean state of tropical SST is a better description of the cause of the shift, rather than changes in El Niño activity. More recently, Kitoh (1991, 1992) and Graham et al. (1993, in preparation) have described atmospheric GCMs forced by anomalies of only tropical SST, only midlatitude SST and global SST, the results of which clearly showed that the midlatitude response over the north Pacific can be excited by tropical SST anomalies alone. Although no clear reason for a step-like tropical ocean change has emerged, intrinsic ocean-atmosphere wave dynamics of the tropics may eventually provide the key.

In this study, we seek to understand the 1976–77 climate shift in the north Pacific Ocean as well as to clarify the importance of the atmosphere in driving low-frequency ocean variability. We use observed anomalies of the surface heat fluxes and wind stresses to force an ocean model constructed with complete physics (but no eddy variability). The ocean model response is free to evolve and is not constrained to reproduce the observed SST or other oceanic variables. We first determine if, given the observed anomalies of heat flux and wind stresses as forcing functions, the ocean model generates observed variations in north Pacific SST, especially those associated with the 1976–77 shift in SST. If such variability is realistically simulated, the ocean model can then provide further insight into the low-frequency anomalous regimes in the ocean-atmosphere system because it contains a history of physical processes that are not available from observations. These results represent the first hindcast of which we are aware that uses observed anomalies of total heat flux and wind stress as forcing for such a long time interval.

We describe in Section 2 (and Appendix A) a layered ocean GCM which we have forced with anomalies of total surface heat flux and wind stress derived from surface marine observations (Sect. 3 and Appendix B). We examine the model upper-ocean variability associated with the 1976–77 climate shift in Section 4 and discuss the physical mechanisms for the shift in Section 5. We summarize the results and discuss their relevance in Section 6.

2 Ocean model

The ocean model was developed by Oberhuber (1993) and consists of eight isopycnal interior ocean layers fully coupled to a surface bulk mixed layer model, the latter also including a sea ice model. The mixed layer has arbitrary density and a minimum depth of 5 m. The interior layers have fixed potential density and time-varying thicknesses (which may vanish) and can intersect the mixed layer or topography as the dynamics allows. The model solves the full primitive equations for mass, velocity, temperature and salt for each layer in spherical geometry with a realistic equation of state. In this study, the domain is the Pacific Ocean with realistic topography, extending from 70°S to 65°N and 120°E to 60°W. The grid resolution is 77 by 67 points, but with enhancement near the equator and near the eastern and western boundaries. Open ocean resolution in the middle latitudes is 4 degrees, which is suitable for modeling the large-scale variability in response that we seek. The conditions on horizontal solid boundaries are no slip for velocity and thermally insulating for temperature. The model Antarctic Circumpolar Current, however, has periodic boundary conditions and unrealistically connects to itself from 60°W to 120°E (half the global circumference). The surface boundary conditions for interior flow are determined by the bulk mixed-layer model which is forced by the atmosphere. Frictional drag acts between each layer but most strongly along the bottom boundary which has realistic topography. Horizontal Laplacian friction with variable coefficients and vertical diffusion (entrainment between layers) is also included. For a full discussion of the dynamics see Oberhuber (1993), who used the model in Atlantic Ocean modeling studies, and Miller et al. (1992), who used an earlier version of this model for tropical Pacific Ocean circulation studies. Appendix A documents the changes invoked between the version studied by Miller et al. (1992) and the version used here.

3 Forcing functions and model runs

Since no ocean model is perfectly realistic, any model forced by observed heat fluxes (without any feedback) will establish an oceanic temperature climatology which will depart from that observed. To circumvent this problem, we have forced the model with observed *anomalies* of heat fluxes (Q') rather than using the complete observed heat flux fields. These observed anomalies are added to a mean heat flux field derived as follows. We first establish the model ocean climatology by forcing with observed long-term monthly mean wind stresses, turbulent kinetic energy (TKE) input and surface heat fluxes computed from bulk formulae using long-term monthly mean atmospheric observations combined with model ocean temperature. After the oceanic system has reached an acceptably equilibrated state, monthly mean fields of the total heat flux ($\bar{Q}$) and sea surface temperature ($\bar{T}_s$) are saved to be

used as forcing input ($Q=\bar{Q}+Q'$) for additional runs which include anomalous observed total heat fluxes.

The observed Q' anomalies should provide the mixed layer heat budget with a good representation of SST *tendency*, as long as heat fluxes dominate SST variability and provided that the model mixed-layer depth represents reality reasonably well. In regions where intrinsic ocean variability dominates the generation of observed flux variability (which generally only occurs over smaller space scales than are of interest in this study, i.e., the ocean mesoscale), however, we would expect poor ocean model results. Insofar that natural ocean feedback processes are much weaker than the atmospheric driving, our results will thus provide a useful measure of understanding the upper-ocean response to atmospheric forcing as long as the model can successfully represent the physical processes involved in evolving such fields as SST and mixed layer depth. Luksch and von Storch (1992) caution that the use of observed air temperature and observed SST in computing even *anomalous* surface heat fluxes for forcing an ocean model can possibly 'build in' the observed SST to the simulation. In our present study, the ocean model does not have any feedback to the observed heat flux anomalies so that this argument does not apply. For example, if the model SST is anomalously warm at a time when observed SST is anomalously cold, the observed fluxes might call for warming of the real ocean which would then result in increasingly warmer (and more erroneous) model SST. The model is clearly free to drift away from observed SST or any other atmospheric field which may constrain SST in nature through ocean feedback processes.

3.1 Spin-up

During an approximately 35-year-long spin-up period, the model was forced (see Oberhuber 1993, for complete details of these forcing fields) by long-term monthly mean fields of atmospheric wind stress τ (interpolated from a blending of ECMWF and Hellerman-Rosenstein analyses), and total surface heat fluxes (latent, sensible long wave radiation and insolation), derived from bulk formulae using *model* SST and long-term observed monthly-mean atmospheric fields of air temperature (from ECMWF analyses), humidity (COADS), wind speed ECMWF) and cloudiness (COADS) as inputs. These long-term mean fields are distinct from the flux and wind stress anomaly fields, formed from individual monthly COADS means by Cayan (1990, 1992a), as discussed later and in Appendix B. The surface (mixed-layer) salinity field is stabilized near the observed climatological average by using Newtonian relaxation to the Levitus annual mean surface salinity (relaxation constant = 5×10^{-6} m/s), instead of using the poorly observed mean evaporation and precipitation (E-P) fields. The salinity in the interior ocean layers is allowed to evolve freely. Although it would be interesting to include E-P anomalies, we presently do not have a long-term set of observations of rainfall variability over the oceans. We should point out, however, that long-term variations in rainfall may have an important effect on the upper ocean density structure and may be related to the climatic shift of 1976–77 which we are attempting to diagnose or to other long-term variations in the oceanic state. Further experiments exploring this effect are therefore warranted.

During the spin-up period, year-to-year changes in SST and MLD (mixed-layer depth) were monitored to help decide if the run had developed a stable and reasonable seasonally varying state (gauged by the smallness of the drift in mean SST and mixed-layer depth, MLD). In general, the response in the north Pacific was much more equilibrated than that in the south Pacific, due mainly to the presence of model sea ice variability in the Antarctic Ocean which apparently requires a longer time scale for equilibration than the upper-ocean of the north Pacific. Over most of the north Pacific, the maximum SST drift was only a few hundreths of a degree from year 34 to year 35 of the spin-up experiments.

After the spin-up period was complete, we stored the monthly mean fields of total surface heat flux, $\bar{Q}$, and SST, $\bar{T}_s$, from the final year of spin-up. The field, $\bar{Q}$, was used as the mean part of the forcing for all the subsequent runs discussed later. To verify that $\bar{Q}$ was sufficient for mean forcing and to allow for initial drifts or adjustments in SST, we ran the model for an additional 5 years with $\bar{Q}$ as the surface heat flux forcing. Since there was little change in mean SST in the north Pacific, we commenced the experiments outlined next from the end of that 5-year period.

3.2 Interdecadal forcing

The wind stress field is composed of the τ used during spin-up, plus monthly-mean anomalies, τ', derived from the COADS observations (Cayan 1990) as follows. In the extra-tropics, the COADS wind stress anomalies are derived from monthly means of the product $|V|V$ from individual wind velocity observations. Drag coefficients were taken from Isemer and Hasse (1987) and are weakly dependent upon wind speed, V, and air-sea temperature difference, ΔT. Since the COADS observations are very lightly sampled in the low latitudes, we used FSU wind stress anomalies (Goldenberg and O'Brien 1981) in the region $\pm20°$ latitude. In an overlap region of approximately 5° latitude at 20°N, the COADS and FSU anomaly fields were smoothly merged.

For the total heat flux anomalies, we adopted a similar strategy. We used Q' as determined by Cayan (1990, 1992a) from the COADS observations poleward of 20° latitude. The COADS latent and sensible fluxes were formed from monthly averages of products of individual observations. Exchange coefficients were taken from Isemer and Hasse (1987) and are weakly dependent on wind speed and ΔT. A sample of the total heat flux anomalies, as seen by the model, is shown in

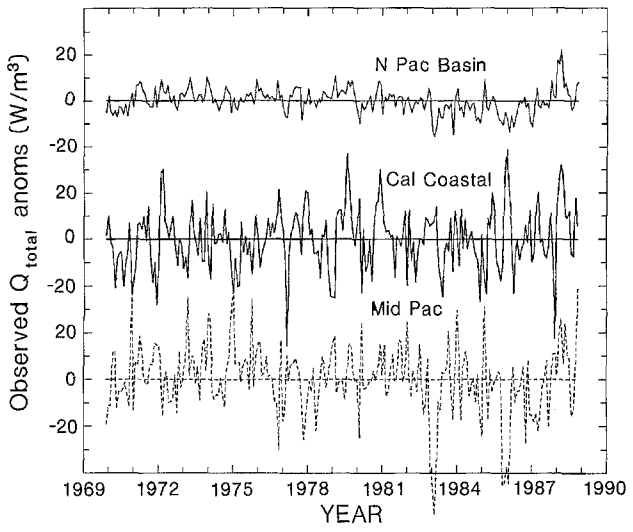

Fig. 1. Observed anomalies of total surface heat flux (latent, sensible, short wave and long wave) as input to the model for Case 1, averaged over key regions. (*Top*) The north Pacific basin wide region: 130°E–110°W and 20°N–60°N, (*middle*) the coastal region: 135°W–120°W and 25°N–45°N, and (*bottom*) the mid-Pacific region: 180°W–150°W and 30°N–40°N. The anomalies (W/m^2) are relative the the 1950–88 mean as computed by Cayan (1990, 1992a) from the COADS. The *horizontal tick marks* correspond to January of the indicated year. An interpolation scheme is used to input the observed 5 by 5 degree data to the model grid, plus a scheme for interpolating in time is used during the time stepping to deal with grid points which have no data for a given month. Note that, particularly for the basin wide region, an extended period of positive heat fluxes (indicative of warming the ocean) occurs during the 1970s. Since it is observed that the 1970s were associated with an anomalously cool ocean state, and because model cases 1 and 2 warm significantly in response to this long-term forcing, we subsequently revised the heat flux calculations for case 3 (see Fig. 3)

Fig. 1. In the low latitudes (±20 degrees latitude), there are many gaps in the ship weather reports so we could not confidently apply the COADS flux anomalies there. We additionally felt it was inappropriate to use the observed Q' in the tropical strip because there is evidence that the main effect of heat fluxes in the tropics is to damp SST anomalies (Liu and Gautier 1990; Cayan 1990; Barnett et al. 1991). Thus, unless the wind-driven model SST reproduced the observed SST with nearly perfect fidelity, the observed Q' would try to damp an SST anomaly that 'wasn't there', resulting in an excitation of model SST anomaly with opposite sign as the observed. We therefore chose to invoke a Newtonian damping scheme for the low latitudes, ±20°, where we let $Q' = \alpha T_s'$, where T_s' is the model SST anomaly, relative to $\bar{T}_s$. The spatially variable constant, α, was determined by analyzing the total heat flux output of the ECHAM T21 atmospheric model run forced, from 1970–85, with observed SST anomalies (Max-Planck-Institut, Hamburg, private communication). The constant, $\alpha(x, y)$, was computed by regressing the observed T' with the ECHAM model's Q' output. Typical values of α vary from $-10\,\mathrm{W\,m^{-2}\,C^{-1}}$ in the eastern tropical Pacific, to near $-40\,\mathrm{W\,m^{-2}\,C^{-1}}$ in the western Pacific (see Barnett et al. 1991, their Fig. 17).

The month-to-month variations of TKE input to the mixed layer are very difficult to estimate from monthly mean observations. However, we felt that it was at least worth an attempt at including the variability since observations show that mean zonal winds increased significantly over the Pacific in the late 1970s. Even a crude parameterization for the increase in TKE input to the mixed layer could help to diagnose the importance of variations in entrainment on the surface temperature budget. Thus, we invoked the Weibull parameterization of Pavia and O'Brien (1986) for relating mean wind speed cubed to monthly mean wind speed of COADS:

$$\{V^3\} = \{V\}^3 \frac{\Gamma(1+3/C)}{\Gamma^3(1+1/C)} \tag{1}$$

where the brackets indicate an average over a given month. Since V is not a vector average, but rather an average of the magnitude of the wind, we feel that the parameterization is reasonable. We chose as a rough estimate, $C=2$, from the north Pacific regions shown by Pavia and O'Brien, which implies that $\{V^3\} \approx 1.9\{V\}^3$. After relating mean cubic wind speed to u_*^3 using eq. (A2) and removing its climatological field, we added the resulting anomalies (see Fig. 2) to the climatological monthly mean u_*^3 (derived from the ECMWF analyses) which were used in the model spin-up period. Note that $(u_*^3)'$ is somewhat correlated with Q' due to the effects of wind speed on Q'. Also note that in the low latitudes (±20°) the estimates are

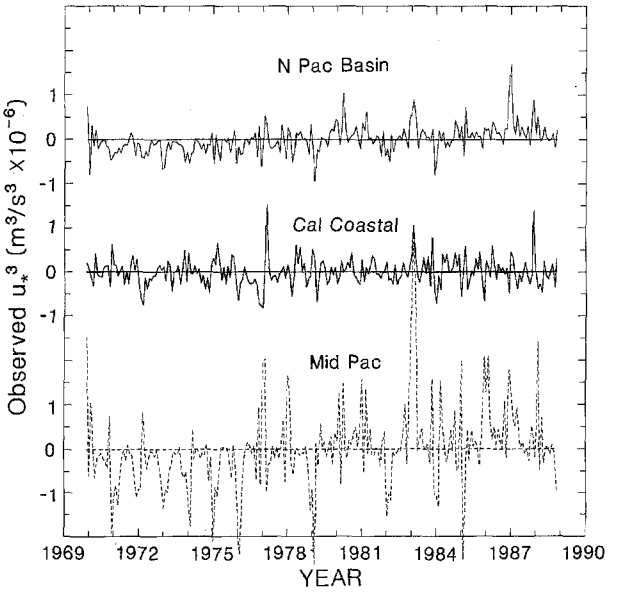

Fig. 2. Estimates of the observed anomalies of u_*^3 (m^3/s^3, scaled by 10^{-6}) as defined by (1) and (A2), relative to the 1950–88 time interval, computed from the COADS; otherwise as in Fig. 1. Negative perturbations are constrained never to exceed 80% of the mean value. Note that, in the mid-Pacific region, there is significantly weaker TKE input during the early 1970s compared to the late 1970s and throughout the 1980s

rather patchy in space and time due to poor data coverage.

3.3 Revision of the observed flux anomalies

We inspected areal averages of the observed north Pacific Q' anomalies (a portion of which are shown in Fig. 1) and noted that long-period fluctuations occur in the COADS observations (see Ramage 1986; Cayan 1990, 1992a; Michaud and Lin 1992). These low-frequency variations result in heat flux anomalies which look very suspicious and would result in unacceptably large shifts of the ocean model climatology over time. Specifically, the marine data contain substantial trends in wind speed, ΔT, and possibly Δq, the humidity differential at the air-sea interface, even when these data are averaged over the largest spatial scales (Cayan 1992a). These are the fundamental variables which affect the bulk formulae fluxes most strongly. The wind speed trends have been noted by several previous authors (Ramage 1986; Cardone et al. 1990; Posmentier et al. 1989) and appear to be instrumental artifacts instead of natural variability. The problems in estimating ΔT from marine data have been noted by Barnett (1984) who attributed the long-period variations to the blending of SST measured by different instrument types (buckets vs. injection). Although we are unable to identify a simple instrumental bias that can directly account for the trends in ΔT and Δq, we have no reason to trust these wholesale decreases in oceanic ΔT and Δq, so we also treat these as spurious variability at the largest spatial scales.

For cases 1 and 2, discussed later, we removed linear trends in both wind speed and ΔT before computing the heat fluxes using bulk formulae. Since that still proved to be inadequate, in case 3 we removed the first empirical orthogonal function (EOF) variability of ΔT and Δq along with a similar, nearly linear trend in wind speed. The resulting heat flux estimates proved satisfactory for the goals of this study. The details of this revision procedure are thoroughly discussed in the Appendix B and examples of its effect are shown in Fig. 3.

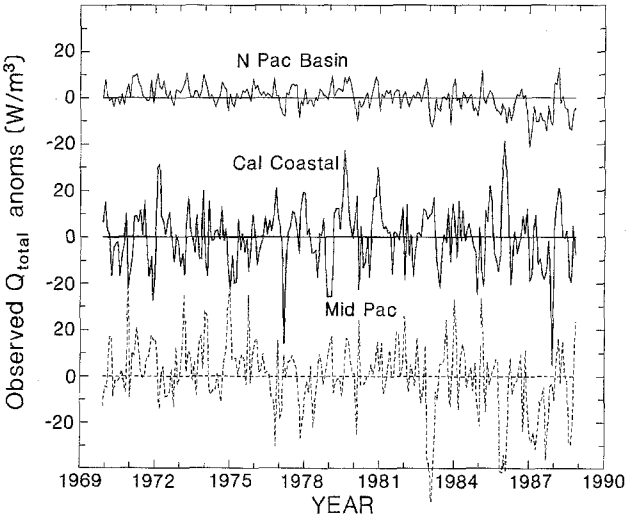

Fig. 3. As in Fig. 1 but for the revised heat-flux anomalies (W/m^2) as input to the ocean model for case 3. These are the resultant 'high-pass' versions of Fig. 1, after using the corrections discussed in Appendix B

3.4 Interdecadal simulations

We consider three basic forcing scenarios, hereinafter referred to as:

case 1 (1965–1988) forced by τ' and Q'
case 2 (1970–1988) forced by τ', TKE$'$ and Q'
case 3 (1970–1988) forced by τ', TKE$'$ and revised Q'

Our first long run, case 1, which commences in 1965 and extends through 1988, uses the Q' and τ' anomaly fields of Section 3.3 as forcing. The second long run, case 2, extends from 1970–1988 and uses these same Q' and τ' fields but also includes our estimates of the month-to-month variability in the TKE fields from Eqs.(1) and (A2) which directly affect the entrainment velocity of the surface mixed layer via (A1). Our third long run, case 3, is forced by the same fields as case 2 but with the revised Q' forcing, 'high-pass' adjusted as discussed in Appendix B to remove the long-period shifts in heat flux which we believe are of questionable reality. As suggested, cases 1 and 2 indeed exhibit long-term shifts in SST with opposite sign to those observed, due to the unfiltered heat flux anomalies. Although cases 1 and 2 are de-emphasized hereinafter, they remain interesting in that can be directly compared to determine the relative efficacy of anomalous TKE in generating SST anomalies. The fundamental results of our analyses for cases 2 and 3 turned out to be quite similar so that the long-term shifts in SST due to the suspicious heat fluxes are probably not contaminating our results.

4 SST response: model versus observations

In order to draw attention to the large-scale variations of the north Pacific, we now focus on two key regions plus a north Pacific basin average. One key region is off the coast of California (designated coastal region), where substantial warming occurred during the 1976–77 climate shift, and is bounded by 135°W–120°W and 25°N–45°N. The other is in the central Pacific (designated by mid-Pacific region), where cooling occurred during the shift, and is bounded by 180°W–150°W and 30°N–40°N. The basin average corresponds to 130°E–110°W and 20°N–60°N.

For a general view of how the model is representing the seasonal thermal variability of the upper ocean, Fig. 4 shows the long-term mean and standard deviations of SST, MLD and the terms of the surface heat budget for case 3, governed by

$$\frac{\partial T_s}{\partial t} + \mathrm{u}\cdot\nabla T_s + \frac{w_e}{H}(T_s - T_o) = \frac{Q}{\rho c_p H} + K\nabla^2 T_s \qquad (2)$$

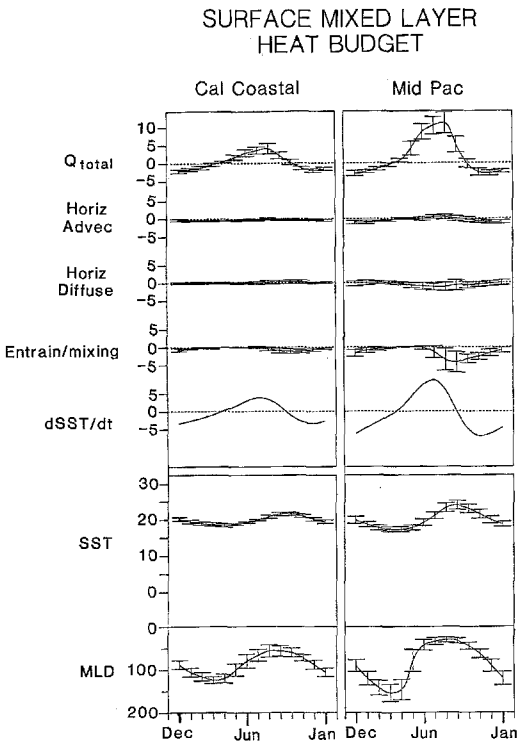

Fig. 4. Climatological monthly mean (*solid lines*) and standard deviation (*vertical bars*) of the terms in the model surface mixed layer heat budget (Eq. 2), averaged over the two key regions. Units are 0.1° C/month for the heat budget terms and SST tendency, ° C for SST and m for MLD. December and January are repeated for clarity

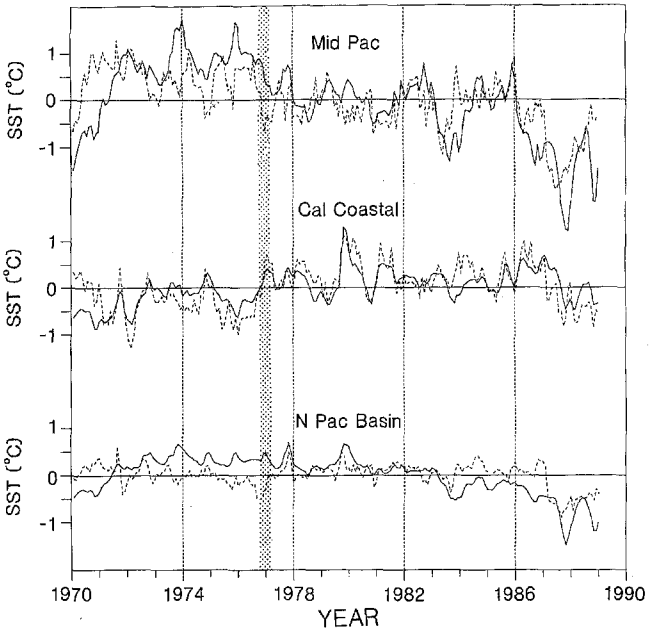

Fig. 5. Time series of observed (*dashed*) and case 3 hindcast (*solid*) SST anomalies (° C) for (*top*) mid-Pacific, (*middle*) coastal and (*bottom*) north Pacific basin wide regions, relative to the 1970–88 respective means. The *horizontal tick marks* correspond to January of the indicated year. The timing of the 1976/77 shift is indicated by the *stippling*. The COADS SST anomalies were filtered with a 1–2-1 filter. The amplitude of typical anomalies is slightly lower for the model than observed. The short term variations in SST, particularly for the coastal region, are surprisingly similar considering the uncertainty in the observed heat-flux, TKE and wind-stress forcing fields. The anomaly correlation coefficients between model and observed are 0.67, 0.71 and 0.44 for the mid-Pacific, coastal and basin wide regions, respectively

where u is the horizontal current, w_e is the entrainment velocity, H is the mixed-layer depth, T_o is the temperature of entrained fluid and K is the spatially variable horizontal diffusivity. We hereinafter refer to the terms in (2) as SST tendency, horizontal advection, vertical mixing/entrainment, heat flux input and horizontal diffusion, respectively. Monthly means of these quantities are computed during the integration from which the climatological monthly means are computed and subtracted from the stored fields to obtain the anomalies. Horizontal averages are then computed over the key regions. The well-known basic features of autumn and winter deepening and spring shoaling of the mixed layer are evident in Fig. 4. Typical anomalies in the depth of the monthly-mean mixed layer, averaged over the key regions, are 10–20 m. Also, the dominance of Q in establishing the mean heat content of the upper ocean (e.g., Gill and Niiler 1973; Barnett 1981) is clearly seen in Fig. 4. Variability in the terms of the heat budget is clearly highest in the winter season. In summary, Fig. 4 shows a midlatitude surface mixed-layer heat budget which is reasonably consistent with what has been observed in nature.

We next examine the nearly two-decade time series of key area averages of model and observed SST anomalies for case 3 shown in Fig. 5. Both model and observed anomalies are defined with respect to their monthly-mean climatology for the 1970–88 time interval. As seen in Fig. 5, both the model and observed SST variability contains activity on monthly, seasonal, annual and decadal time scales. Over the entire north Pacific, the model exhibits a long term variation in SST which is not evident in the observations and is likely a residual effect of the long-term variation of heat flux as described earlier. The longer time scale variability in the two key regions, in contrast, correlates quite well with the observations.

The shorter period model SST variability in Fig. 5 has many features in common with the observed, particularly for the coastal region. The correlation coefficients between the model and observed SST time series in the coastal and mid-Pacific regions are 0.71 and 0.67, respectively. These must be viewed with caution since the SST contains variability on all time scales and correlation is biased towards representing the time scales with the greatest variance; thus, the correlation values represent some weighted average of the model's ability to model shorter and longer term variations, including model drift. Highlighted by stippling in Fig. 5, the 1976–77 warming observed in the coastal region is evident in the model's response, as is the 1976–77 cooling of the mid-Pacific region. Note that the 1976–77 shift is only subtlely evident when inspecting the time series in Fig. 5 because they include *all* months; the shift is readily seen when focusing on the winter months alone.

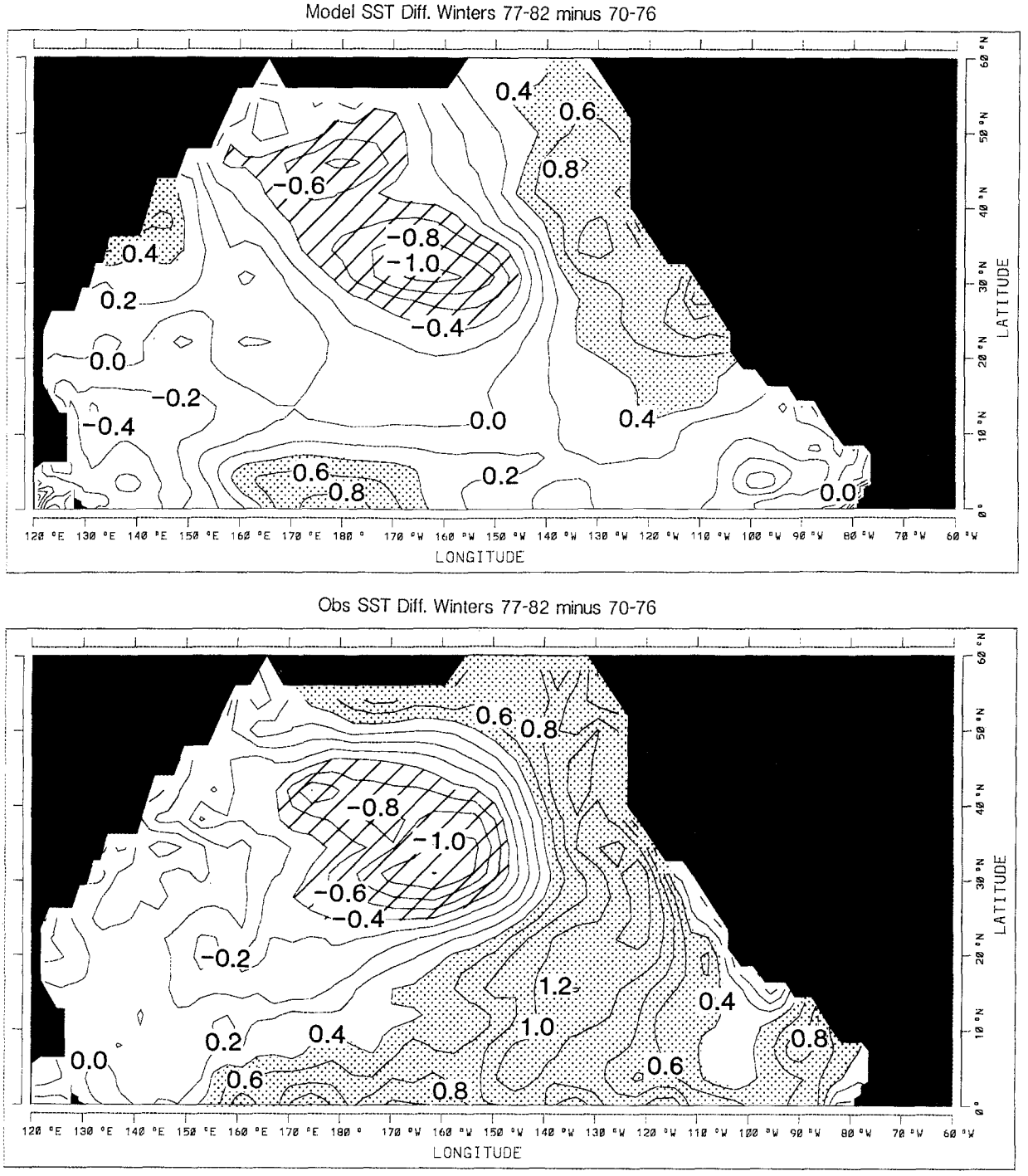

Fig. 6. Difference field of winter time (DJF) SST (°C) for the 1976/77 through 1981/82 winters minus the 1970–71 through 1975–76 winters for (*top*) model case 3 hindcast and (*bottom*) COADS observed. The large-scale pattern of mid-Pacific cooling and coastal warming has been captured by the model. Warming in the western equatorial Pacific has also been reproduced but the warming observed along the eastern part of the tropics does not occur in the model, apparently due to the Newtonian heat flux procedure which is invoked in the tropical strip (±20° latitude)

To better reveal the spatial pattern of the model SST response to the 1976–77 winter time shift, we calculate the difference between SST after the shift and SST before the shift. Following Graham (1991), Fig. 6a shows the winter time SST difference field for the six years after the shift (Dec 1976–Feb 1977 through Dec 1981–Feb 1982) minus the six years before the shift (Dec 1970–Feb 1971 through Dec 1975–Feb 1976). For comparison, the same field derived from observations is shown in Fig. 6b. (Note that other chosen multi-year intervals around the shift lead to similar results, but our choice leaves out the strong signal of the 1982–83 El Niño and thus provides a sharper criterion for capturing the shift. Note also that the first two years of the

experiment seem to be influenced by poor initial conditions from case 1, i.e., SST anomalies are initially one-degree too cold.) As seen in Fig. 6, case 3 captures the essential feature of the observations, namely a warming in the coastal region and a cooling in the mid-Pacific region, although the modeled coastal region does not warm as much as in nature. The other feature of the observations is a swath of warm water across the southeastern north Pacific and throughout the equatorial region. The model results exhibit a vestige of the swath, but the model equatorial Pacific region only shows a warming in the western half of the tropics. Since the model includes Newtonian damping rather than observed fluxes in the tropical strip we are not too surprised by the discrepancy. The modeled warming in the equatorial Pacific points to possible dynamic effects of warming due to wind stress anomalies alone, since tropical air temperature increases are not essential to cause SST warming in that important region of the tropics. This model result thus suggests that tropical air-sea interaction may be more important than air temperature increases (e.g., due to greenhouse gas emissions) in generating the observed warming of tropical SST.

Case 2 has a 0.3° C warmer shift in the coastal region and 0.3° C weaker cool shift in the mid-Pacific region. This is clearly due to our removing in case 3 the longterm warming effects of the COADS during the 1970s, as discussed previously. The mid-Pacific cool shift is weaker in case 1 compared to case 2, evidently due to the lack of anomalous TKE input to the mixed layer.

To gain insight on the large-scale patterns of SST variability we show in Fig. 7 the EOFs of the entire time series for the north Pacific in both model and COADS. The largest scale pattern seen in EOF-1 of the SST observations is also evident in the model EOF-1. Discrepancies include a displacement of the maximum amplitude roughly 10° southwards, too little warming in far eastern basin, somewhat weaker amplitude than observed and a much greater percentage of the SST variance being associated with it. The time variability of model and observed EOF-1 has a 0.66 correlation, but the general feature of the 1976–77 shift is only weakly present. The second EOF of the model and observed SST anomalies corresponds only fairly well to each other in space and time (correlation 0.36), with the model again underpredicting variability north of about 45° N. The climate shift of 1976–77 is clearly evident in the time series of the observed EOF-2, but is less strongly apparent in the model analogue time series. The third EOF of the model and observations appears to be unrelated in spatial and temporal content (correlation 0.04).

To focus on the winter time when the heat fluxes and wind stresses are highest in mean and variability, we also present a winter EOF analysis in Fig. 8. This shows EOFs for only the winter seasons, averages of December, January and February, i.e., just 19 points. Here, the comparison of model and observations is remarkable, considering the difficulty in modeling the

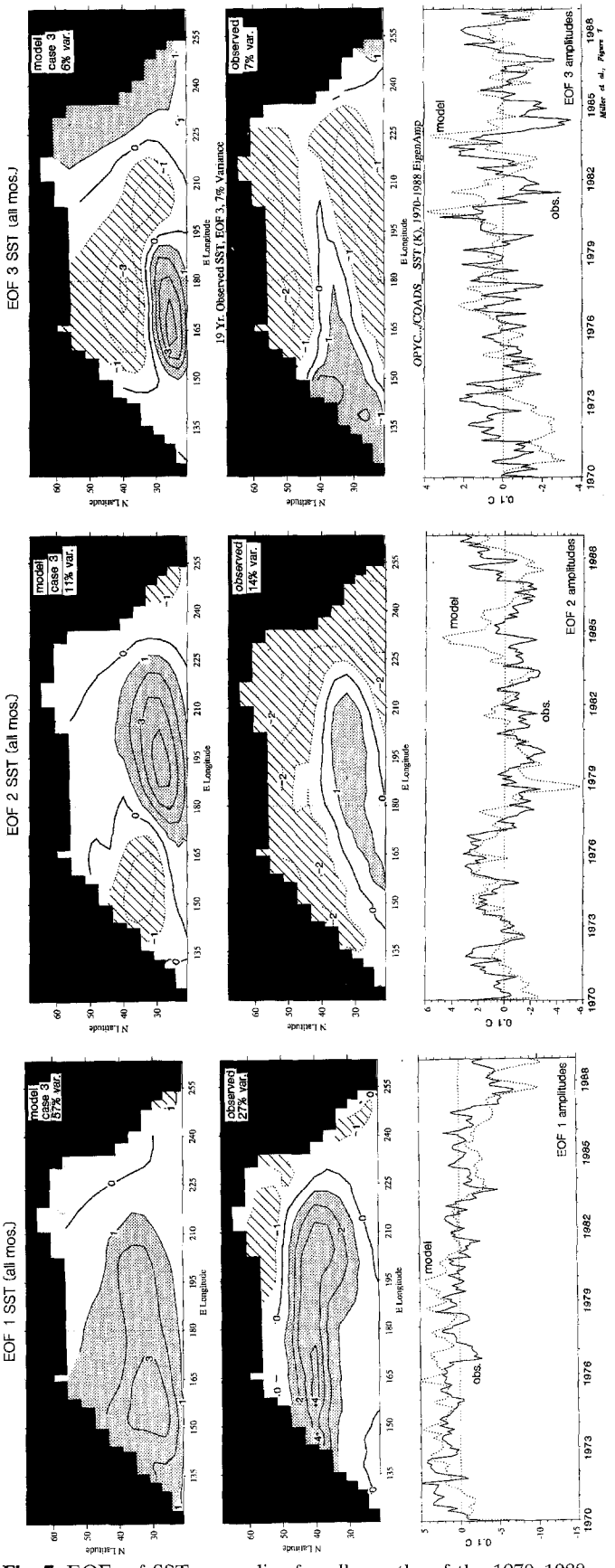

Fig. 7. EOFs of SST anomalies for all months of the 1970–1988 time interval for (*top*) model case 3 hindcast and (*middle*) COADS observations. (*Bottom*) Time series of the EOF coefficients for model and observations. The correlations between the model and observed time series are 0.66, 0.36 and 0.04, respectively

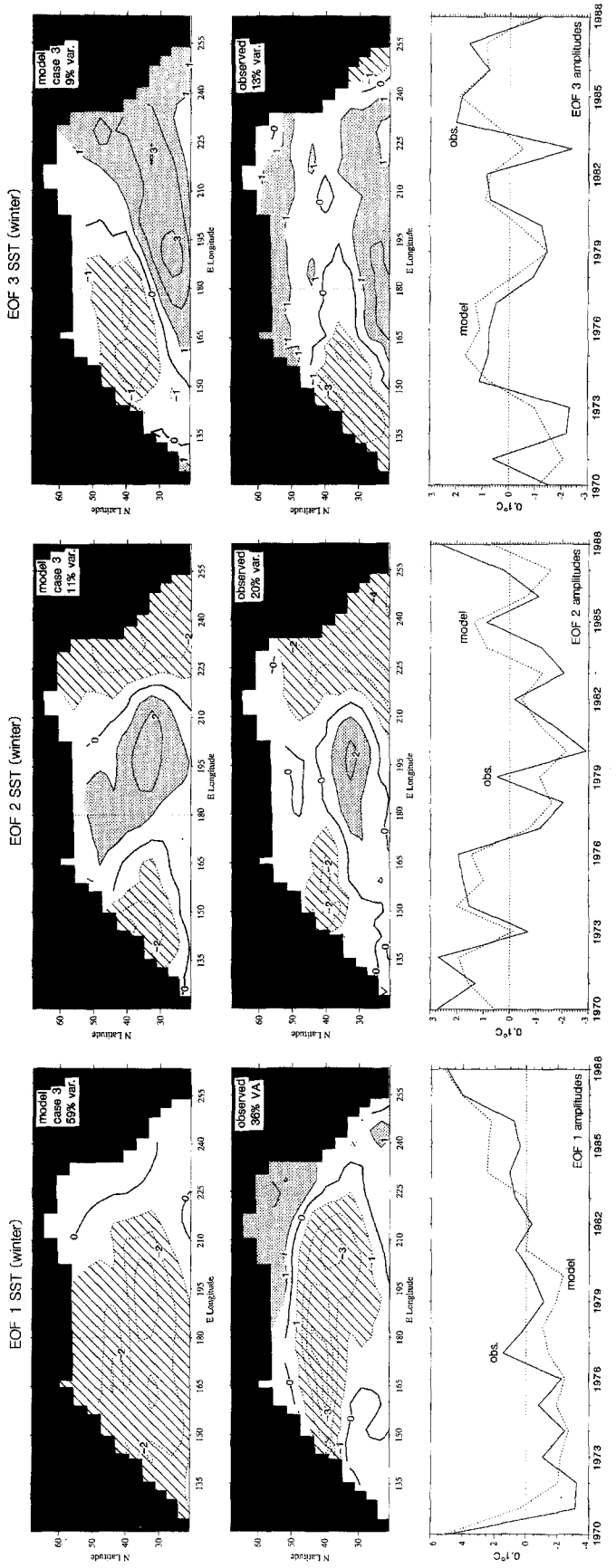

Fig. 8. As in Fig. 7 but for winter (DJF) seasons of the 1970–1988 interval. The degree of correspondence between modeled and observed EOF spatial structure and time variability is remarkable. The correlations between model and observed time series are 0.83, 0.78 and 0.74, respectively

oceanic seasonal cycle over a basin scale combined with the considerable uncertainty in the heat-flux and wind-stress observations. The spatial similarity between the model and observed EOFs is much closer for the winter time fields than for the year-round monthly fields. Furthermore, the time variability of the EOFs compares surprisingly well among the model and observed, showing correlations of 0.83, 0.78 and 0.74 for the first three EOFs. The 1976–77 shift is weakly evident in the first EOF and strongly represented in the second EOF for both model and COADS. The relative importance of the EOFs in describing the total SST variance, however, is more variable; the three model EOFs describe 59, 11, and 9% of the variance, compared to the three observed EOF describing 36, 20 and 13%. These winter EOF results suggest that since the forcing signal is stronger in winter, the signal in the response is stronger as well. Also, the model is less sensitive to errors in the forcing in winter because the MLD is deeper and hence less easily erroneously perturbed (as a percentage of total depth) than the thin mixed layers of summer.

We have thus found that this ocean model is capable of generating a shift in mid-latitude SST similar to that observed, when forced by observed anomalies of total heat flux and wind stress. Furthermore, much of the time variability of the model SST fields compares well with the observed in the sense of reproducing large-scale patterns (EOFs) and regional averages. The good agreement in winter is particularly important because winter is the period when the anomalous extratropical forcing is strongest. We, therefore, proceed with an analysis of the mixed layer heat budget to attempt to determine the reasons why the 1976–77 shift in oceanic SST occurred and to study further the relative importance of terms in the heat budget which excite large-scale SST anomalies.

5 Mechanisms of SST variability

To determine what physical processes caused the 1976–77 shift in the mid-latitudes, we examine the time variability of the anomalies of the terms in the surface mixed-layer heat budget (Eq. 2), as well as MLD anomalies, surface heat flux anomalies and SST anomalies.

Inspection of the differences in amplitude of the anomalous driving and damping terms of the heat budget (e.g., Figs. 4, 9, 10) reveals that heat flux input tends to be the largest anomalous forcing term, in line with results of previous studies (e.g., Gill and Niiler 1973; Frankignoul 1985; Haney 1985; Luksch et al. 1990; Luksch and von Storch 1992). In the coastal region (Fig. 9), typical heat flux input anomalies tend to be about four times larger than the anomalous effects of either horizontal advection or entrainment. In the mid-Pacific region (Fig. 10), in contrast, which is nearer the stronger and more variable winds of the storm track (e.g., Haney et al. 1981), the anomalous effect of heat flux input is only twice as large as that of horizon-

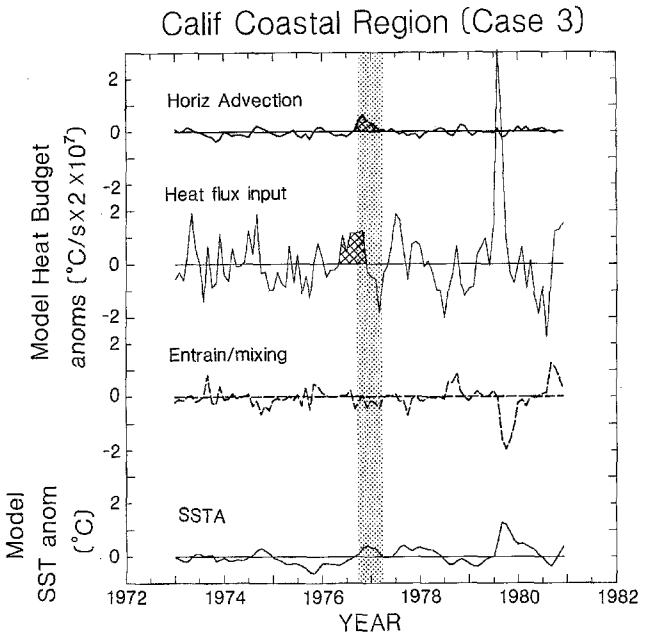

Fig. 9. Time series of monthly-mean anomalies in the mixed-layer heat budget (*top three curves:* °C/s, scaled by 0.2×10^{-8}), and (*bottom*) SST anomalies (° C) from the model hindcast case 3 for the 1973–1980 interval in the California coastal region. The heat budget terms are for variations in horizontal advection, heat-flux input and vertical mixing/entrainment. Anomalies are computed with respect to the entire 1970–1988 interval. There is very little difference in the results for case 2 compared to case 3. The cause of the 1976–77 climate sift (*highlighted by stippling*) is due to a unique occurrence of warming by strong horizontal advection anomalies combined with persistent heat-flux input anomalies for a multi-month interval preceding the winter time shift (both indicated by hatching)

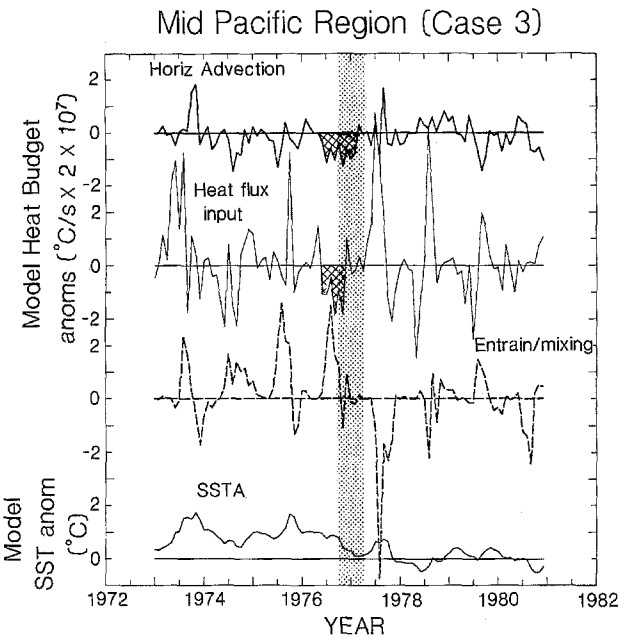

Fig. 10. As in Fig. 9, but for the mid-Pacific region. The cause of the 1976–77 climate shift (*stippling*) is due to a unique occurrance of cooling by strong and persistent horizontal advection anomalies combined with persistent heat-flux input anomalies for a multi-month interval preceding the wintertime shift (*both indicated by hatching*). The maintenance effects of weaker vertical mixing (*dashed line*) before the shift and stronger mixing afterwards are also evident. Other large forcing events tend to be either too short-lived or counterbalanced to have an important long-term effect on SST

tal advection and roughly the same size as entrainment effects. Although anomalous diffusion is only slightly weaker than horizontal advection, diffusion acts mainly in opposition to the heat flux input terms. Since its effect is passive (smoothing out SST anomalies which were mainly excited by the other terms), we discuss diffusion no further.

During the six month period preceding the 1976–77 climate shift, Fig. 9 shows that the coastal region experienced a long period of warming via heat flux input. Although the anomalous heat flux driving during this period was not particularly strong, it was persistent compared to most of the rest of the time intervals. What makes this period particularly unique, however, is that the strongest event (of the 1970–88 time interval) of warming by horizontal advection occurs during fall 1976 and the subsequent winter. These two effects taken together result in a 10–15 m shallower mixed layer and more than half a degree warming in the surface temperature.

In the mid-Pacific region, the 1976–77 climate shift is likewise instigated by the synergistic effects of an anomalously long and strong period of cooling by horizontal advection combined with sizable cooling by heat flux input (Fig. 10). The MLD anomalies change from being 10–20 m shallower before the shift to being 10–15 m anomalously deeper after the shift, a roughly 30 m swing. During the persistent cooling event, anomalous SST drops approximately 1° C.

Note that many of the sporadic large events in forcing the surface heat budget seen in Figs. 9 and 10 occur during summer when the mixed layer is thin and therefore much less influential in affecting SST in subsequent seasons. Furthermore, they are often too short-lived or counterbalanced by other large events to have a significant long-term impact on the SST. The sustained anomalies in horizontal advection and surface heat flux in fall 1976 and winter 1976–77 are unique.

By inspecting the years before and after the shift, we can ascertain mechanisms for the maintainance of the two interdecadal climatic states. Figure 10 suggests that, in the mid-Pacific region, the period before the shift is marked by anomalously weak entrainment effects (mainly due to lower TKE input as seen in Fig. 2) followed by stronger entrainment effects afterwards. This tendency is corroborated by Fig. 11 which shows the difference in SST between case 2 and case 1 and clarifies the importance of long-term variations in vertical mixing as the dominant maintainance effect in the mid-Pacific region. The direct effect of including TKE anomalies in Eq. (2) is to cause SST to be warmer in the early 1970s and cooler in the late 1970s and 1980s. During the 5-year interval around the 1976–77 shift, however, the vertical mixing effects are relatively constant, supporting the interpretation that the step-like

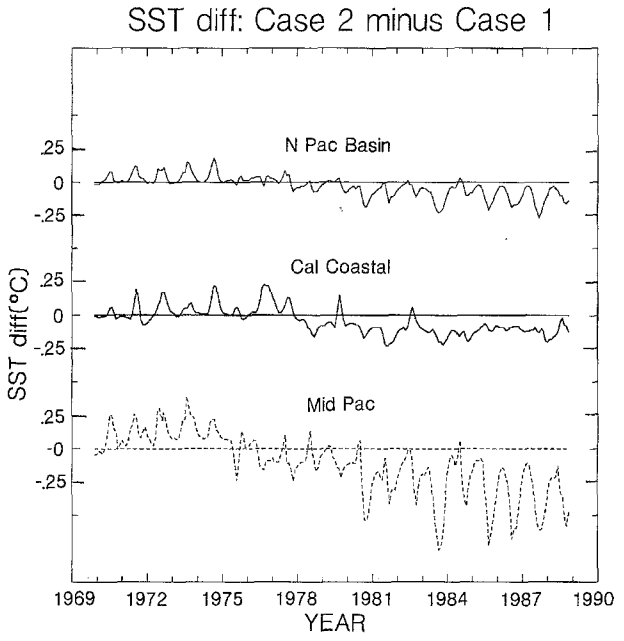

Fig. 11. Differences in monthly-mean SST between case 2 and case 1 simulations, showing the direct effects of including variable TKE input to the bulk mixed layer for the (*top*) north Pacific basin-wide, (*middle*) California coastal and (*bottom*) mid-Pacific regions. Although TKE anomalies are largest in winter (Fig. 2), the effects are felt most strongly in the other seasons when the depth of the mixed layer is shallower

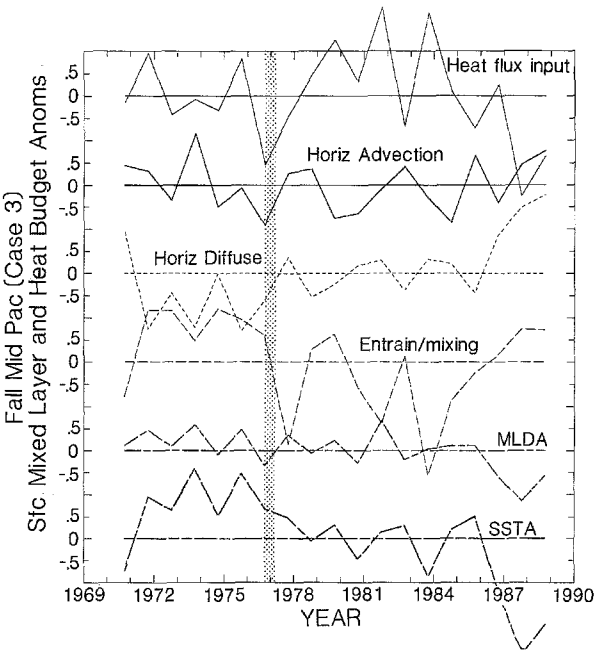

Fig. 12. As in Fig. 10, but for fall (SON) seasons only in the mid-Pacific region. (*Top to bottom*) The four heat budget terms (heat-flux input, horizontal advection, horizontal diffusion and vertical mixing/entrainment; scaled as in Fig. 9), mixed-layer depth (m, scaled by 0.1) and SST anomalies (°C). The fall season maintainence effect of anomalous vertical mixing is clearly visible in this plot. The other terms in the heat budget do not exhibit a consistent fall season maintainence effect before or after the shift

shift is maintained but not directly caused by variations in mixing.

For a sharper image of the seasonal variations of the heat budget terms, Fig. 12 shows the fall anomalies and Fig. 13 shows the winter anomalies for the mid-Pacific region during for the entire integration. The strong effects of cooling by advection and heat flux input are clearly evident in the fall of 1976, as is the maintainence effect of the fall entrainment anomalies in anomalously warming the region before the shift and cooling it after the shift. The effects of fall activity on the subsequent winter conditions is evident in Fig. 13 which shows an anomalously shallow mixed layer in the winters before the shift and deeper thereafter. Thus, the transition from fall to winter season is a key point in understanding the occurrence of the anomalous winter state (e.g., Namias 1976; Davis 1978); anomalous entrainment events in the fall lead to corresponding changes in winter MLD and SST, the persistence of which is well known (e.g., Namias et al. 1988).

In the coastal region, in contrast, there is no maintainance effect of entrainment variations of SST evident in Fig. 11. If we look for what might cause a stronger maintainence effect in the monthly-mean heat budget time series, we find no clear long-term persistent effect of warming after the 1976–77 shift. However, in the heat budget time series stratified by season (not shown), winter time heat flux input does exhibit a consistent trend of anomalous cooling before the shift and warming afterwards. Weaker effects of anomalous

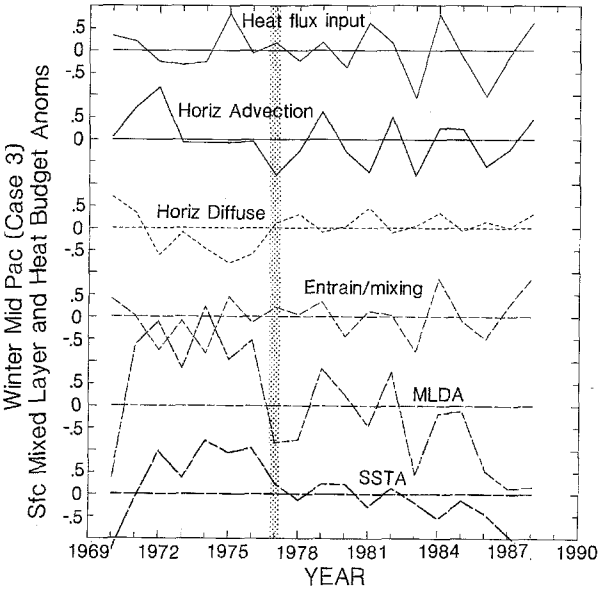

Fig. 13. As in Fig. 12, but for winter (DJF) seasons only. The winter mixed layer is clearly shallower before the shift and deeper afterwards and is correlated to the SST anomaly. The MLD anomalies result from preconditioning by the fall vertical mixing anomalies; the four terms in the heat budget do not exhibit a consistent maintainence effect during winter seasons before or after the 1976–77 shift in the mid-Pacific region

entrainment also appear to help support the interdecadal states during the fall seasons.

It therefore appears that the 1976–77 shift in both the coastal and mid-Pacific regions was caused by an unique atmospheric state which persisted for many months before and during the 1976–77 winter. The uniqueness of the atmospheric state was that it resulted in large-scale shifts in ocean current advection which acted in concert with large-scale heat transfer processes to significantly alter the upper-ocean thermal structure. The mid-Pacific region remained in the two different climatic states through maintainence effects of prolonged changes in the flux of atmospheric momentum (TKE input) into the mixed layer, contributing to a deeper winter mixed layer in the mid-Pacific after the shift. The maintainence of the coastal region is less clear but appears to be more strongly influenced by direct heat flux forcing. Our model depiction of events is consistent with the ocean modeling results discussed by Haney (1980), for the September 1976 through January 1977 time interval, who showed that SST warming in the eastern Pacific was predominantly due to anomalous heat fluxes and that central Pacific SST cooling was strongly influenced by anomalous Ekman currents.

6 Summary and discussion

We have integrated an ocean GCM over a nineteen-year time interval using observed anomalies of heat fluxes, wind stress and TKE input in order to diagnose the physical mechanisms in the ocean which led to the significant climate shift of the winter of 1976–77 as well as to understand mechanisms for other long-term variations in SST. The model successfully reproduced the 1976–77 shift in winter time SST, as well as other large-scale SST variability throughout the time interval.

We have found that two mechanisms acting in concert thrust the system into a different state. During a many-month period preceding and during the shift, very large horizontal advective effects collaborated with normal-sized but long-lived heat flux input variations to produce mid-Pacific cooling and California coastal warming (compare with Haney 1980). Although these two effects caused the shift in the mid-Pacific region, prolonged changes in the flux of atmospheric momentum to the ocean (vertical mixing variations) maintained it.

It is, therefore, of interest to turn attention to the atmospheric fields themselves to discern what motivates and maintains the shift. Cayan (1992c) has shown that monthly mean heat flux anomalies are organized in large-scale patterns which have strong influence on the ocean thermal structure. A more difficult question is to what extent these ocean thermal anomalies, once initiated, act to modify the air-sea heat exchange and hence affect the atmospheric circulation (e.g., Cayan 1992b; Alexander 1992). These patterns could be related to persistent regimes of mid-latitude ocean-atmosphere interaction (Namias 1963; Palmer and Sun 1985; Namias et al. 1988; Miller 1992) whereby feedback effects of heat transfer maintain the atmospheric thermal field and wind stresses maintain the ocean SST fields, each in their persistent state.

Since the ocean model does not contain feedback to the atmosphere and it succeeds in capturing the major features of the 1976–77 shift, the results suggest that the midlatitude part of the shift was driven by the atmosphere. However, if ocean-atmosphere feedback did occur in nature its effect is implicitly included in the observed heat flux anomalies used to drive the model so that important effects of midlatitude ocean-atmosphere feedback can be masked and may yet be identified. The question of whether the atmospheric shift is generated locally in the midlatitude or remotely (via teleconnections) from the tropics has been addressed by Kitoh (1991, 1992) and Graham et al. (1993) in recent experiments using atmospheric models forced by SST anomalies. These model runs indicate that the 1976–77 shift of the atmosphere in the midlatitudes is driven remotely by a contemporaneous shift in tropical Pacific SST and commensurate changes in deep tropical convection.

Another interesting point which can be drawn from this study is the relative importance of heat flux input, horizontal advection and vertical mixing effects on open ocean SST anomaly generation in this model. Previous ocean modeling studies by Haney et al. (1978), Huang (1979), Haney (1980, 1985), Luksch et al. (1990) and Luksch and van Storch (1992) and coupled ocean-atmosphere modeling studies by Miller (1992) and Tokioka et al. (1992) have shown the general tendency for strong effects of anomalous heat fluxes and lesser, though not insignificant, influences of horizontal advection and vertical mixing on the generation of midlatitude SST anomalies. We have found that in the mid-Pacific region heat-flux input and entrainment tend to typically have similarly sized anomalous forcing effects on the surface heat budget of the variable depth mixed layer (Figs. 4 and 10); horizontal advection effects are typically half that size. In the region near the California coast, the winds are less variable and the entrainment and horizontal advection effects on the heat budget tend to be only about one-quarter the size of heat flux input anomalies (see Haney 1980; Luksch and von Storch 1992). In contrast to our results, Luksch and von Storch (1992) found that the effects of turbulent mixing on the surface heat budget was small, but their heat budget corresponds to the surface grid point of a z-coordinate model rather than to the entire mixed layer in the present model. Figure 11 shows that, under the assumption that our parameterization for monthly-mean TKE′ input is reasonable, monthly mean SST anomalies generated by the effects of vertical mixing/entrainment variations can be more than 0.5° C, in general agreement with the results of Haney (1985). Note that although winter time TKE anomalies are largest (Fig. 2), the impact on the mixed layer heat budget (Fig. 10) is felt most strongly in other seasons when the depth of the mixed layer is shallower.

These suggestions are corroborated by the results of a companion study of the case 3 simulation by Cayan et al. (1993) who discussed point-by-point spatial correlations between the driving terms of the surface heat budget (Eq. 2) and SST tendency. Their results show that over the bulk of the north Pacific the heat flux input indeed correlates strongly (>0.6) with SST tendency. However, over a large region of the north-central and north-eastern Pacific, advection correlates at levels greater than 0.4. The effects of entrainment also correlate well with SST tendency (>0.5) over surprisingly large regions of the north Pacific basin, particularly in a latitudinal belt across 25°N. Their results also show that in the tropical Pacific the wind stress driving produces high correlations between observed and model SST (greater than 0.8 between 160°W–170°W) suggesting that the version of the model studied here indeed represents an improvement over the earlier version studied by Miller et al. (1992).

We summarize lastly some of the potential defects of the ocean modeling approach which was used here. The effects of horizontal advection, which rely strongly on the horizontal gradients of the mean SST, may be underestimated by two effects. First, the climatological field of model SST tends have gradients which are somewhat weak compared to observation, especially in the northwest Pacific. Second, the horizontal velocity anomalies in the surface mixed layer are weaker than surface (i.e., zero meters depth) currents and are not representative of the shears which can exist in the mixed layer, because they correspond to velocity anomalies in the entire bulk mixed layer. However, the model surface currents will correctly represent the Ekman transport which is presumably the most important bulk effect of anomalous ocean currents (e.g., Gill and Niiler 1973). The model also does not contain mesoscale eddies or properly resolve the Kuroshio Current and, therefore, does not have the ability to generate such effects as strong currents in the western boundary region which could conceivably swiftly introduce SST anomalies in open ocean regions, though they are probably of too small spatial scale and amplitude to be of consequence (Klein and Hua 1988; Halliwell and Cornillon 1989; Miller 1992). But the gentler effects of large-scale wind forced geostrophic current advection should be well represented by the model. There is also a roughly 4° C warm bias in the model winter time SST field in the northern reaches of the Pacific basin which may result in a stratification structure which is too stable to allow stronger effects of entrainment variations. Also, the south Pacific basin had many patches of SST variations associated with the long adjustment times of ice variations (near the Antarctic) and slow changes in the thermal structure yielding sometimes abrupt shifts in MLD. Future modeling studies may be necessary to address these potential difficulties.

Acknowledgements. Support was provided by NOAA Grants NA16RC0076-01 and NA90-AAD-CP526, NASA Grant NAG5-236, the G. Unger Vetlesen Foundation and the University of California INCOR program for Global Climate Change. AJM also acknowledges the hospitality and support of the Institute of Geophysics and Planetary Physics of the Los Alamos National Laboratories where he commenced this research while he was an Orson Anderson Visiting Scholar. Supercomputing resources were provided by the National Science Foundation through the National Center for Atmospheric Research and the San Diego Supercomputer Center. AJM thanks Sho Nakamoto for paraphrasing the Kashiwabara (1987) article. For constructive comments on the manuscript we thank Ute Luksch, Michael Alexander and the two referees.

Appendix A

Details of the isopycnic ocean model

The isopycnic ocean model (Oberhuber 1993) used in this study differs from that used by Miller et al. (1992; MOGB, hereinafter) in basin geometry, forcing functions and the following details. A potential vorticity and enstrophy conserving horizontal finite differencing scheme, based on that derived by Bleck and Boudra (1981), is implemented in this version of the model. Since MOGB found that the mixed layer depth in the midlatitudes was much deeper than observations, we sought to tune the present version of the model to yield a more realistic seasonally varying mixed layer depth (see Fig. 4). To accomplish this, two important things were changed in the equation for entrainment velocity:

$$w_e g' h - w_e Ri_{crit}(\Delta u^2 + \Delta v^2) = 2 m_o a u_*^3 + h b (B - \gamma B_s) + \gamma b B_s [h(1 + e^{-h/h_B}) - 2 h_B (1 - e^{-h/h_B})] \quad \text{(A1)}$$

where g' is the reduced gravity at the mixed layer base, $Ri_{crit} = 0.25$, $(\Delta u, \Delta v)$ is the velocity jump at the base of the mixed layer, $m_0 = 0.5$, $a = \exp(-hf/\kappa u_*)$, $b = \exp(-hf/\kappa u_*)$ for all values of the buoyancy flux B, $\gamma = 0.42$, B_s is the solar buoyancy flux, and $h_B = 20$ m. First, the amplitude of the mean turbulent kinetic energy (TKE) input into the mixed layer was reduced by setting $m_o = 0.5$, rather than 1.5 in MOBG, and additionally

$$u_*^3 = \left(\frac{c_d \rho_a}{\rho}\right)^{\frac{3}{2}} [(\bar{V})^3 + (\overline{V^3})'], \quad \text{(A2)}$$

which does *not* have a mean correction term based on the standard deviation of the mean wind speed that was invoked in MOGB. In (A2), $(\bar{V})^3$ is the climatological monthly mean wind speed and represents the mean term while $(\overline{V^3})'$ is the anomalous cube of the monthly mean wind speed, the estimation of which is discussed in Section 3.2. Second, this version of the model has $\kappa = 0.4$, a constant value, rather than increasing for $B > 0$ as in MOGB. This effect controls the strength of cold air outbreaks originating from Asia and allows the mixed layer to deepen sufficiently well in the winter season. Note that in the computation of B_s, only the climatological monthly mean values of the solar heat flux are used in (2). The net result of our tuning is to reduce the MLD in the middle and high latitudes of the north Pacific relative to that of MOGB, with the present values being more typical of those ob-

served (Barnett 1981; Levitus 1982; Suga and Hanawa 1990).

Appendix B

Technique for revising the heat flux anomalies

We made two attempts to remove the suspicious time-varying changes in the fundamental variables involved in the computation of the heat flux. Following Cayan (1990; 1992a), our first attempt was to calculate the area-averaged linear trend of wind speed and ΔT, where the area considered was the entire COADS data coverage over the global ocean. Then, the equivalent latent and sensible heat flux change was computed for each month of each 5° by 5° grid point, by adding the linear change in V and ΔT to their respective long-term monthly means and inserting these into the two bulk formulae. By subtracting the long-term monthly mean flux value from each month of the 1950–1988 time history, a "correction" to the latent and sensible fluxes was obtained to reduce the apparent time-varying bias. The anomalies of these fluxes (e.g., Fig. 1) were used to force cases 1 and 2 of the experiments described in the text.

This procedure, however, still proved unsatisfactory in that there remained apparently spurious low-frequency changes in the flux component of the forcing. Further inspection indicated three problems. First, the time varying bias for ΔT, which generally decreases over time, was *not* linear, but undergoes substantial low-frequency undulations over the period since 1950. This is in contrast to the wind speed, which exhibits a clear linear increase of about 1 m/s change over 1950–88. Second, there also appear undulations in Δq, similar to ΔT, which were not accounted for in the initial trend adjustment. Third, the effect of changes in ΔT upon the net outgoing terrestrial flux was not accounted for in the original correction (this was because the initial flux anomaly study focused on variations in the latent and sensible components rather than the net flux).

In the second flux adjustment procedure, we attempted to more accurately remove the basin-scale low-frequency variation (generally decreasing) of ΔT and include an adjustment for similar variation (also generally decreasing) in Δq, while retaining the adjustment for V increases. The flux "correction" was calculated in the same manner as before by perturbing the long-term mean data entering the bulk formulae with the time varying coefficients. However, in this case, the adjustments to ΔT, Δq and V were determined from a basin-scale empirical orthogonal function (EOF), rather than from a linear trend. The EOF analysis was performed on a smoothed version (13-month running mean filter applied twice) of the three COADS data fields encompassing the Pacific basin from 30°S to 60°N and 130°E to 75°W. In each of the three smoothed variables, the spatial pattern of the first EOF exhibited one sign over virtually the entire field. Further, the time coefficients for the first EOFs contained the time variation that was generally portrayed by the linear trend (V increasing and ΔT and Δq decreasing), as shown in Fig. A1. The first EOFs accounted for 55%, 43% and 73% of the smoothed ΔT, Δq and V fields respectively. The projection of the first EOF back onto the smoothed data constituted the time varying adjustments that were then applied to ΔT and Δq in computing the flux corrections. Since the first EOF of the smoothed wind speed was very nearly linear and showed relatively little spatial variation, we did not readjust the COADS wind stress anomalies, which were corrected using the original COADS global average linear trend of 0.8 m/s over 1950–1988. These adjustments were applied to the respective bulk formulae for the latent, sensible and net terrestrial (infrared) heat fluxes. The anomalies from this second version of the corrected fluxes (Fig. 3 vis-a-vis Fig. 1) were employed in case 3.

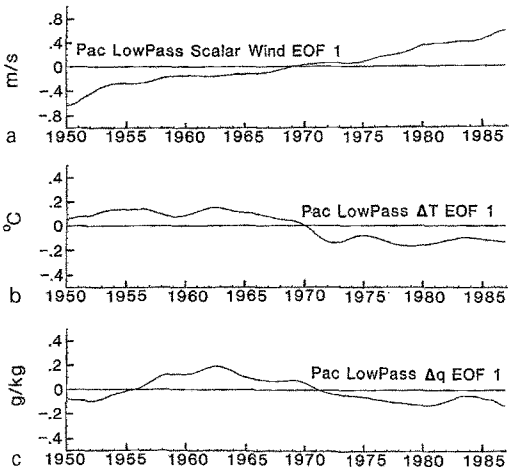

Fig. A1. Time series of the coefficients of first EOFs of low-pass filtered monthly mean **a** wind speed, V, **b** air-sea temperature difference, ΔT, and **c** air-sea interface humidity differential, Δq, over the north Pacific. The first EOFs of **b** ad **c** were applied as corrections to the bulk formulae heat flux calculations for case 3. A linear trend was retained as the correction for V

References

Alexander MA (1990) Simulation of the response of the North Pacific Ocean to the anomalous atmospheric circulation associated with El Niño. Clim Dyn 5:53–65

Alexander MA (1992) Midlatitude atmosphere-ocean interaction during El Nino. Part I: the north Pacific Ocean and part II: the Northern Hemisphere atmosphere. J Clim 5:944–972

Barnett TP (1981) On the nature and causes of large-scale thermal variability in the central North Pacific Ocean. J Phys Oceanogr 11:887–904

Barnett TP (1984) Long term trends in surface temperature over the oceans. Mon Weather Rev 112:303–312

Barnett TP, Latif M, Kirk E, Roeckner (1991) On ENSO physics. J Clim 4:487–515

Bleck R, Boudra DB (1981) Initial testing of a numerical ocean circulation model using a hybrid coordinate (quasi-isopycnic) vertical coordinate. J Phys Oceanogr 11:755–770

Bjerknes J (1969) Atmospheric teleconnections from the equatorial Pacific. Mon Weather Rev 97:163–172
Cardone VJ, Greenwood JG, Cane MA (1990) On trends in historical marine data. J Clim 3:113–127
Cayan DR (1990) Variability of latent and sensible heat fluxes over the oceans. PhD. Dissertation, University of California, San Diego
Cayan DR (1992a) Variability of latent and sensible heat fluxes estimated using bulk formulae. Atmos Ocean 30:1–42
Cayan DR (1992b) Latent and sensible heat flux anomalies over the northern oceans: the connection to monthly atmospheric forcing. J Clim 5:354–369
Cayan DR (1992c) Latent and sensible heat flux anomalies over the northern oceans: driving the sea surface temperature. J Phys Oceanogr 22:859–881
Cayan DR, Miller AJ, Barnett TP, Graham NE, Ritchie JN, Oberhuber JM (1993) A two-decade simulation of the Pacific Ocean forced by observed monthly surface marine observations. In: Climate von decade-to-century time scales. National Academy of Sciences press, Washington DC, 20418 (in press)
Davis RE (1978) Predictability of sea level pressure anomalies over the north Pacific Ocean. J Phys Oceanogr 8:233–246
Douglas AV, Cayan DR, Namias J (1982) Large-scale changes in north Pacific and North American weather patterns in recent decades. Mon Weather Rev 110:1851–1862
Ebbesmeyer CC, Cayan DR, McLain DR, Nichols FH, Peterson DH, Redmond KT (1991) 1976 step in the Pacific climate: forty environmental changes between 1968–75 and 1977–1984. In: Betancourt JL, Tharp VL (eds) Proceedings of the 7th Annual Pacific Climate (PACLIM) Workshop, California Department of Water Resources, Interagency Ecological Studies Program Technical Report 26
Folland CK, Parker DE, Kates FE (1984) Worldwide marine temperature fluctuations 1856–1981. Nature 310:670–673
Frankignoul C (1985) Sea surface temperature anomalies, planetary waves, and air-sea feed-back in the mittle latitudes. Rev Geophys 23:357–390
Gaffen DJ, Barnett TP, Elliot WP (1991) Space and time scales of global tropospheric moisture. J Clim 4:989–1008
Gill AE, Niiler PP (1973) The theory of the seasonal variability in the ocean. Deep-Sea Res 20:141–177
Goldenberg SB, O'Brien JJ (1981) Time and space variability of tropical pacific wind stress. J Phys Oceanogr 11:1190–1207
Graham NE (1991) Decadal-scale climate variability in the 1970s and 1980s: Obervations and model results. In: Proceedings of the Fifteenth Annual Climate Diagnostic Workshop, US Department of Commerce/NOAA/NWS/NMC/CAC PB91-171082
Graham NE (1993) Decadal-scale climate variability in the 1970s and 1980s: observations and model results. Clim Dyn (in press)
Graham NE, Barnett TP, Schlese U, Bengtsson L (1993) On the roles of tropical and midlatitude SSTs in forcing interannual to interdecadal variability in the winter Northern Hemisphere circulation. Manuscript in preparation
Halliwell GR, Cornillon P (1989) Large-scale SST anomalies associated with subtropical fronts in the western North Atlantic during FASINEX. J Mar Res 47:757–775
Haney RL (1980) A numerical case study of the development of large-scale thermal anomalies in the central north Pacific Ocean. J Phys Oceanogr 10:541–556
Haney RL (1985) Midlatitude sea surface temperature anomalies: a numerical hindcast. J Phys Oceanogr 15:787–799
Haney RL, Shriver WS, Hunt KH (1978) A dynamical-numerical study of the formation and evolution of large-scale ocean anomalies. J Phys Oceanogr 8:952–969
Haney RL, Risch MS, Heise GC (1981) Wind forcing due to synoptic storm activity over the north Pacific Ocean. Atmos Ocean 19 (2):128–147
Horel JD, Wallace JM (1981) Planetary scale atmospheric phenomena associated with the Southern Oscillation. Mon Weather Rev 109:813–829
Huang JCK (1979) Numerical case studies for ocean thermal anomalies with a dynamical model. J Geophys Res 84:5717–5726
Isemer H-J, Hasse L (1987) The Bunker Climate Atlas of the North Atlantic Ocean. Vol. 2: air-sea interactions. Springer, Berlin Heidelberg New York
Kashiwabara T (1987) On the recent winter cooling in the North Pacific. Tenki 34:777–781 (in Japanese)
Kitoh A (1991) Interannual variations in an atmospheric GCM forced by the 1970–1989 SST. Part II: low-frequency variability of the winter time Northern Hemisphere extratropics. J Meteorol Soc Japan 69:271–291
Kitoh A (1992) Decade-scale interannual variations simulated in an atmospheric GCM using the observed 1970–1989 SST. In: Progress in climate study – report of the Japanese National Projects for WCRP 1987–1991 (in press)
Klein P, Hua BL (1988) Mesoscale heterogeneity of the wind-driven mixed layer: influence of a quasigeostrophic flow. J Mar Res 46:495–525
Levitus S (1982) Climatological atlas of the World Ocea. US Department of Commerce, NOAA Prof Pap 13
Liu WT, Gautier C (1990) Thermal forcing on the tropical Pacific from satellite data. J Geophys Res 95:13209–13217
Luksch U, von Storch H, Maier-Reimer E (1990) Modeling North Pacific SST anomalies as a response to anomalous atmospheric forcing. J Mar Syst 1:155–168
Luksch U, von Storch H (1992) Modeling the low-frequency sea surface temperature variability in the North Pacific. J Clim 5:893–906
McLain DR (1983) Coastal ocean warming in the Northeast Pacific, 1976–1983. In: Pearcy WG (ed) The influence of ocean conditions on the production of salmonids in the North Pacific. Oregon State University, Sea Grant Program, ORESU-W-83-001
Michaud R, Lin CA (1992) Monthly summaries of merchant ship surface marine observations and implication for climate variability studies. Clim Dyn 7:45–55
Miller AJ (1992) Large-scale ocean-atmosphere interactions in a simplified coupled model of the midlatitude winter time circulation. J Atmos Sci 49:273–286
Miller AJ, Oberhuber JM, Graham NE, Barnett TP (1992) Tropical Pacific Ocean response to observed winds in a layered general circulation model. J Geophys Res 97:7317–7340
Namias J (1963) Large-scale air-sea interactions over the North Pacific from the summer 1962 through the subsequent winter. J Geophys Res 68:6171–6186
Namias J (1976) Negative ocean-air feedback systems over the North Pacific in the transition from warm to cold seasons. Mon Weather Rev 104:1107–1121
Namias J (1978) Multiple causes of the North American abnormal winter 1976–77. Mon Weather Rev 106:279–295
Namias J, Yuan X, Cayan DR (1988) Persistence of North Pacific sea surface temperature and atmospheric flow patterns. J Clim 1:682–703
Nitta T, Yamada S (1989) Recent warming of tropical sea surface temperature and its relationship to the Northern Hemisphere circulation. J Meteorol Soc Japan 67:375–383
Oberhuber JM (1993) Simulation of the Atlantic circulation with a coupled sea ice – mixed layer – isopycnal general circulation model. Part I: model description and part II: model experiment. J Phys Oceanogr 22:808–845
Palmer TN, Sun Z (1985) A modelling and observational study of the relationship between sea surface temperature in the northwest Atlantic and the atmospheric general circulation. Quart J R Meteorol Soc 111:947–975
Pavia EG, O'Brien JJ (1986) Weibull statistics of wind speed over the ocean. J Clim Appl Meteorol 25:1324–1332

Peixoto JP, Oort AH (1992) The physics of climate. American Institute of Physics, New York

Posmentier ES, Cane MA, Zebiak SE (1989) Tropical Pacific trends since 1960. J Clim 2:731–736

Ramage CS (1986) A comparative analysis of marine records from ocean weather stations and merchants-ships. In: Woodruff SD (ed) Proceedings of a COADS Workshop, NOAA Techn Memo ERL ESG-23

Seymour RJ, Strange RR, Cayan DR, Nathan RA (1984) Influence of El Niños on California's wave climate. In: Proceedings of the 19th International Conference on Coastal Engineering, American Society of Coastal engineering, Houston

Suga T, Hanawa K (1990) The mixed-layer climatology in the northwestern part of the North Pacific subtropical gyre and the formation area of subtropical mode water. J Mar Res 48:543–566

Tanimoto Y, Iwasaka N, Hanawa K, Toba Y (1992) Characteristics variations of sea surface temperature with multiple time scales in the North Pacific. J Clim (sub judice)

Trenberth KE (1990) Recent observed interdecadal climate changes in the Northern Hemisphere. Bull Am Meteorol Soc 71:988–993

Tokioka T, Kitoh A, Nakagawa S (1992) Relationships between monthly mean sea surface temperature anomalies and sea level pressure anomalies realized in a coupled atmosphere-ocean general circulation model. In: 2nd Int Conf on Modelling Global Climate Change and Variability (Abstr), 7–11 Sep 1992, MPI Hamburg

Venrick EL, McGowan JA, Cayan DR, Hayward TL (1987) Climate and chlorophyll a: long-term trends in the central North Pacific Ocean. Science 238:70–72

Xu J-S (1992) The joint normal modes of the coupled atmosphere-ocean system observed from 1967–1986. Max-Planck-Institut für Meteorologie, Hamburg, Rep no 78